

General Disclaimer

One or more of the Following Statements may affect this Document

- This document has been reproduced from the best copy furnished by the organizational source. It is being released in the interest of making available as much information as possible.
- This document may contain data, which exceeds the sheet parameters. It was furnished in this condition by the organizational source and is the best copy available.
- This document may contain tone-on-tone or color graphs, charts and/or pictures, which have been reproduced in black and white.
- This document is paginated as submitted by the original source.
- Portions of this document are not fully legible due to the historical nature of some of the material. However, it is the best reproduction available from the original submission.

X-616-68-454

PREPRINT

NASA TM X-63409

BOW SHOCK ASSOCIATED WAVES OBSERVED IN THE FAR UPSTREAM INTERPLANETARY MEDIUM

D. H. FAIRFIELD

NOVEMBER 1968

70078



GODDARD SPACE FLIGHT CENTER
GREENBELT, MARYLAND

FACILITY FORM 602

_____	N 69-17995	_____
(ACCESSION NUMBER)		(THRU)
<i>42</i>		<i>1</i>
(PAGES)		(CODE)
NASA-TMX-63409		<i>29</i>
(NASA CR OR TMX OR AD NUMBER)		(CATEGORY)



X-616-68-454

**BOW SHOCK ASSOCIATED WAVES OBSERVED IN THE
FAR UPSTREAM INTERPLANETARY MEDIUM**

**D. H. Fairfield
Laboratory for Space Sciences
NASA-Goddard Space Flight Center
Greenbelt, Maryland**

November 1968

Extraterrestrial Physics Branch Preprint Series

BOW SHOCK ASSOCIATED WAVES OBSERVED IN THE
FAR UPSTREAM INTERPLANETARY MEDIUM

D. H. Fairfield

Laboratory for Space Sciences
NASA-Goddard Space Flight Center
Greenbelt, Maryland

Abstract

Fifty orbits of Explorer 34 data have been used to study .01-05hz transverse waves in the interplanetary medium region between the bow shock and the spacecraft apogee of $34 R_E$. It is concluded that the waves are associated with the earth's bow shock since they only occur when projection of the interplanetary field observed at the spacecraft intersects the shock. The waves are observed 18.5% of the time when a total of 134 days of interplanetary data is considered, but more than 90% of the time when the field has the proper orientation with respect to the bow shock. On the basis of this result it is suggested that these waves with 20-100 second periods are a permanent feature of the solar wind-earth interaction. The transverse component of the waves is typically several gammas in amplitude in 4-8 gamma fields. The disturbance vector in the XY plane generally exhibits the same sense of rotation in a coordinate system where the field is oriented along the positive z axis. Attenuation of wave amplitudes with distance from the bow shock is estimated to be only a factor of two when the spacecraft is $15 R_E$ from the bow shock. The absence of waves at particular field orientations, even though the field line

intersects the shock, is interpreted as a propagation effect. This observation is the basis for calculations which yield an average propagation velocity in the plasma frame of 2.7 ± 0.4 times the solar wind velocity. Whistler propagation and local generation by two stream instability are discussed as alternate theoretical explanations for the presence of the waves. It is suggested that the data favor the latter mechanism.

1. Introduction

Early spacecraft measurements (Ness et al, 1964; Wolfe et al, 1966) revealed the presence of the earth's bow shock as the surface separating the undisturbed interplanetary medium from the thermalized solar plasma and enhanced fluctuating magnetic fields of the magnetosheath. More recent refined measurements, however, have disclosed phenomena in the upstream interplanetary region which are associated with the presence of the earth. Fan et al, (1964, 1966), Anderson (1968) and Jokipii (1968) have studied 30-40 kev electron bursts in the upstream region which may be 10's of earth radii from the bow shock. Vela spacecraft orbiting rather near the shock at $18 R_E$ have observed protons intermittently flowing from the bow shock into the solar wind (Asbridge et al., 1968). These protons have energies greater than those of solar wind protons and energy densities which sometimes are an appreciable fraction of the solar wind energy density. Frank (1968) has observed similar proton events at greater distances from the shock on higher apogee spacecraft.

Heppner (1967) has reported small amplitude waves in the magnetic field in close proximity to the bow shock at frequencies predominantly near 1 hz and sometimes greater than 7 hz. Greenstadt et al. (1968) have used a searchcoil magnetometer on the Vela spacecraft near the shock to detect disturbances with

periods 20-60 seconds in a plane perpendicular to the spacecraft spin axis.

The work reported here utilizes Explorer 34 vector magnetic field data to extend the analysis of these waves in the period range of 20-60 seconds. It will be demonstrated that: (1) the waves are transverse fluctuations with amplitudes which are a sizeable fraction of the total ambient field strength; (2) the waves are associated with the bow shock even though they are observed at distances 10's of earth radii from it;

(3) wave frequencies are below the proton gyrofrequency and tend to be larger in stronger fields; (4) the waves tend to be circularly polarized with a preferred sense of rotation; and (5) the waves have an average velocity in the plasma frame between 2 and 3 times the solar wind velocity. The waves appear to be the transverse fluctuations discovered by Kawashima (1968) in IMP II data and the waves with greater than 10 second periods noted by Jokipii (1968) in IMP I data, even though the 20 second sampling frequency on these spacecraft was not rapid enough to uniquely reveal the characteristics of these waves.

II. Explorer 34 Magnetic Field Experiment

The Explorer 34 (IMP F) spacecraft was launched from the western test range at 14:06 UT May 24, 1967 into an eccentric polar orbit with apogee near the ecliptic plane. Initial perigee of the spacecraft was 278 km, apogee 211024 km ($34.1 R_E$ geocentric), inclination 67.4° and period 4 days, 7 hours and 45 minutes. The spacecraft is spin stabilized and the initial spin period was 2.587 seconds. The orbit is shown in Figure 1 with the upper portion exhibiting the projection in the XY solar ecliptic plane and the lower portion the YZ projection. The apogee at launch was near 1900 hours local time so that during the 7 month period after launch the motion of the earth around the sun caused the apogee of the spacecraft to sweep across the sunlit hemisphere, permitting measurements to be made in the interplanetary medium.

The magnetic field experiment on Explorer 34 consists of a triaxial fluxgate magnetometer with sensor ranges of $\pm 32\gamma$ or $\pm 128\gamma$. The range was changed by ground command twice each orbit at pre-selected times so as to keep the instrument in its optimum range. The analog sensor outputs were digitized onboard the spacecraft with a digitization error of $\pm .16\gamma$ and $\pm .64\gamma$ in the low and high ranges respectively. The sensors were mounted on two six-foot booms with one sensor parallel to the spin axis on one boom and two orthogonal sensors perpendicular to the spin axis on the opposite boom. The spin of the spacecraft was utilized in making an in-flight determination of the zero levels on the sensors perpendicular to the spin axis.

Every 3.9 days the sensor parallel to the spin axis was automatically "flipped" 180° to provide a check on its zero level. Every two hours throughout the flight, checks were made on the perpendicular sensors and the zero levels were observed to be stable within 1.0γ and 0.3γ during the first 9 months of the flight. These zero levels are determined to an accuracy estimated as $\pm 0.1\gamma$. The accuracy of the zero level of the sensor parallel to the spin axis is estimated as $\pm 0.3\gamma$.

Vector field measurements were made every 2.556 seconds with the three individual sensors being sampled sequentially at 80 millisecond intervals. In addition to the normal vector sampling on Explorer 34, an onboard autocorrelation computer was utilized to obtain higher frequency power spectra information. One sensor was sampled every 80 milliseconds and 240 digitized values were supplied to the autocorrelation computer which computes 9 lagged products that are subsequently transmitted to the ground. Taking the fourier transform of this autocorrelation function then yields 9 estimates of the power spectrum below the 6.25 Hz cutoff frequency. This information can be used to ascertain whether the 2.5 second vector samples are aliased. The bandpass of the magnetometers was 0-10 Hz in the low range with a falloff of 20 db/decade in amplitude response beyond 10 Hz.

III. Results

The waves investigated in this paper are observed during portions of all of the first 50 orbits when the spacecraft is in the upstream solar wind region between the bow shock and satellite apogee.

Wave Characteristics

Figure 2 shows a typical example of coherent waves observed in the interplanetary medium at a position ($X_{SE}=20.5$, $Y_{SE}=20.3$, $Z_{SE}=2.7R_E$) $14 R_E$ from the average bow shock location. Wave amplitudes are typical and are of the order of a few gammas compared to the average field magnitude of 5.6γ . Figure 3 shows an example of some less coherent waves which were observed adjacent to the bow shock at the position $X_{SE}=7.1$, $Y_{SE}=17.8$, $Z_{SE}=7.7$. The greater irregularity of these wave forms and somewhat larger wave amplitudes are typical of a region within a few earth radii of the shock.

A polarization diagram for the data between 0457 and 0459 of Figure 2 is shown in Figure 4. Points on this figure represent the locus of successive 2.556 sec. XY data points in a coordinate system where the average field is in the Z direction which is directed into the page. The arrows on the connecting lines of Figure 4 indicate the counterclockwise sense of rotation. The phase lag between the XY components in this field oriented coordinate system was computed for more than 70 half-hour intervals. In more than half of these cases there existed a high enough coherence between the X and Y components to determine a meaningful phase lag. Approximately 90% of the time the phase lag in this

field oriented coordinate system was near 90° corresponding to the counterclockwise rotation illustrated in Figure 4. This was true in spite of variations of the polarity of the field relative to the shock. A few occurrences of 270° phase lag corresponding to the opposite sense of rotation were found with the clearest cases coming from a twelve hour interval on November 6, 1967.

Power spectra were determined for the 70 half-hour intervals when waves were occurring. Generally, half-hour intervals were analyzed with 60 spectral estimates and 23 degrees of freedom. Typical spectra are shown in Figure 5 for the field magnitude and three components in the coordinate system where Z is the average field direction for the interval and X and Y are the orthogonal components with X lying in the plane formed by Z and the earth-sun line. The four traces are offset by one decade in power. Greater spacing between the Y and Z traces is typical of all spectra and is indicative of enhanced power in the transverse components, thus establishing that the waves are primarily transverse fluctuations.

The enhanced power is particularly large in the frequency range .01-.05 Hz. This region is below the proton gyrofrequency; although, as can be seen in the figures, some enhanced power remains at frequencies above the proton gyrofrequency. Since the spacecraft measurements are made in a coordinate system moving at the solar wind velocity with respect to the plasma frame, the measurements will be doppler shifted from their plasma frame values. The spectra of

Figure 5 are typical, although often there is a more pronounced spectral peak in the region with periods between 20 seconds and one minute.

Occurrence Properties

The occurrence of these waves as a function of field direction and spacecraft position has been studied extensively using 134.6 days of interplanetary data from the first 50 orbits of Explorer 34. The presence or absence of the waves is usually easily determined by visual examination of plots of the 2.556 second data points. Plots of the first fifty orbits were scanned and intervals of wave occurrence were noted ranging in length from a few minutes to several hours. The waves were present 18.5% of the time the spacecraft was in the interplanetary medium but only for particular field orientations relative to the spacecraft and the bow shock.

Figure 6 shows the presence of waves as a function of field orientation. The rectangles of Figure 6 represent equal solid angle regions on the solar ecliptic sphere at the latitude (θ) and longitude (ϕ) positions indicated. Using the 8-point (20.5 second) field averages, the number of field occurrences in each directional interval were calculated when the waves were present. In addition, the number of occurrences was determined for the entire set of interplanetary

data and the ratio of cases with waves to total cases was determined for each directional interval. These ratios when multiplied by 100 indicate the percentage of the time the waves occurred in each directional interval and are the numbers presented in Figure 6. This figure shows interplanetary data for orbits 36-40 at which time the satellite was in the solar ecliptic longitude region between 298° and 318° . The numbers in Figure 6 show that for fields of certain orientations the waves occur as much as 92% of the time while for other orientations they do not occur at all. The presence of waves is occasionally undetected when unusually disturbed ambient interplanetary fields occur, so 92% is actually the lower limit to the frequency of occurrence. When one considers the position of the spacecraft on these five orbits, it is evident that the waves tend to be observed when the projection of the magnetic field line at the spacecraft intersects the bow shock.

This point is further demonstrated in Figure 7. The preparation of this figure involved compilation of data from successive five-orbit intervals in the form of Figure 6. Waves were seen less often at Explorer 34 for fields oriented further from the ecliptic plane (see Figure 6), so the latitude dependence was suppressed and only data from the equatorial regions ($-10.8 < \theta < 10.8$) was used to construct Figure 7. In this figure each trace represents the percentage occurrence of waves as a function of longitude for the five-orbit time intervals designated. The horizontal bars

represent the range of ϕ angles of fields measured at the average satellite position which would intersect an average shock. The vertical dashed lines indicate the ϕ angle at which a field would be oriented perpendicular to the shock. The double peak in each trace of Figure 7 is due to fields with the same orientation but opposite direction. The two peaks for each orbital interval are symmetrically oriented within the accuracy of the data and indicate that the sense of the field (toward or away from the shock) is not important in the occurrence of waves. Figure 7 indicates that the waves are observed only when a field line connects the spacecraft and shock. The observation of waves is critically dependent on spacecraft position relative to the shock since the waves are almost always seen at $\phi=140^\circ$ and 320° on orbits 45-50 but virtually never seen at the same ϕ angles, on orbits 1-5 where the orientation with respect to the shock is approximately 90° different. This result is interpreted as indicating that waves must be associated with the shock and not a property of the undisturbed interplanetary medium. Furthermore, the waves do not appear to propagate isotropically since they are only observed on field lines which intersect the shock.

Propagation Velocity

Although Figure 7 shows that a field line must connect the satellite and the shock in order that the waves be seen, close examination shows that the converse is not true and there are

certain field orientations connecting spacecraft and shock at which the waves are generally never seen. In particular, notice $60^\circ < \phi < 85^\circ$ on orbits 46-50; $80^\circ < \phi < 105^\circ$ on orbits 41-45; $100^\circ < \phi < 125^\circ$ on orbits 36-40; $245^\circ < \phi < 275^\circ$ on orbits 6-10. The situation is represented schematically in Figure 8 where ϕ_w represents the ϕ interval where waves are seen, and angle $BA'B'$ the interval where they are not seen. The absence of waves at these orientations can be explained by assuming that the wave phenomena propagate along field lines and by considering the transit time from shock to spacecraft. In Figure 8, a magnetic field line (AB) convected radially from the sun with the solar wind velocity is shown at the instant it first encounters the shock. If the wave phenomenon starts propagating upstream at this time, $t=0$, it will travel distance AB in the time $V_w t$ where V_w is the velocity of the phenomenon in the plasma frame of reference. During this time interval point A is convecting towards the earth and at time t the field line is represented by line $A'B'$. If the orientation of line AB is at the critical angle ϕ_c with respect to the earth-sun line such that the wave is just able to reach the satellite in time t , we may write $AA' = V_{sw} t$ where V_{sw} is the solar wind velocity. If the field has an orientation with ϕ slightly greater than ϕ_c , the wave cannot reach the spacecraft position in time t . Combining the equations $AB = V_w t$ and $AA' = V_{sw} t$ yields $V_w = \frac{AB}{AA'} V_{sw}$. This equation gives the wave velocity in

the plasma frame as a function of the distance AB and AA' which are determined by the spacecraft position and the angle ϕ_c . The relatively sharp cutoff of the occurrence of waves in Figure 7 means that ϕ_c can be determined and this equation used to obtain a velocity. This velocity has been calculated for each of the five-orbit intervals and the results are shown in Table 1. Also shown in the table are AB, AA' and ϕ_c , which were determined from the data of Figure 8 along with the data from off the equatorial plane. The average plasma frame velocity calculated from the values in Table 1 is $2.7 V_{sw}$ with an uncertainty of $\pm 0.4 V_{sw}$.

Attenuation Characteristics

One of the outstanding characteristics of bow-shock associated waves detected by Explorer 34 is their occurrence at large distances from the shock. The waves are detected somewhat less frequently when the spacecraft is more than $25 R_E$ from the earth but only because the range of field orientations where waves are seen is smaller. For a particular field direction where waves are observed, the waves are seen just as frequently beyond $25 R_E$ as inside $25 R_E$, thus demonstrating that over a distance of the order of $15 R_E$ the waves are not damped to the extent that they are unrecognizable.

A systematic study of wave amplitude or power as a function of distance from the shock is difficult but some insight may be gained by studying standard deviations of the field components

computed over an interval which is comparable to the periods of the waves. The specific quantity which has been investigated as an indicator of wave amplitude is $\bar{\delta} = \frac{1}{3} (\delta_x + \delta_y + \delta_z)$ where δ_i are the conventional component standard deviations $\delta_i = \left(\frac{1}{7} \sum_{j=1}^8 (x_j - \bar{x})^2 \right)^{\frac{1}{2}}$ with x_j indicating a solar ecliptic vector component and the 8-point interval being one telemetry sequence of 20.5 seconds. The quantity $\bar{\delta}$ was computed for three categories of interplanetary data: (1) no waves present; (2) waves beyond 25 R_E ; and (3) waves within 25 R_E . With no waves present, a value $\bar{\delta} = .31\gamma$ was found which may be attributed to instrumental digitization and ambient interplanetary field fluctuations and discontinuities. With waves present, $\bar{\delta}$ increased to $0.89\gamma (R < 25 R_E)$ and $0.56\gamma (R > 25 R_E)$. These numbers suggest that attenuation over a distance of 15 R_E is not much greater than a factor of 2.

Further evidence for long distance propagation of bow shock associated waves is obtained by examining data from Explorer 33 which has an apogee of nearly 80 R_E . Although this spacecraft has a lower sampling rate (5.11 second intervals) and less sensitivity, ($\pm .25\gamma$ digitization error) evidence of the waves may still be found far from the bow shock. Figure 9 shows 20 minutes of Explorer 33 data on Feb. 19, 1967 when the spacecraft is 46 R_E from the average shock position. Although quantization noise is more apparent than on Explorer 34, a waveform of the type seen at Explorer 34 is present in the data but with reduced amplitude.

The reduced amplitude of the waves at Explorer 33 precludes the unambiguous identification of all wave intervals and therefore prevents a statistical study such as that accomplished with Explorer 34 data; however, numerous examples of waves near the Explorer 33 apogee have been detected.

Effect on Field Magnitudes

The interplanetary field magnitude might be expected to be different when waves are present and when they are absent. To investigate this possibility, Figure 10 has been prepared where the relative number of occurrences of 20.45 second average fields in half gamma intervals has been plotted vs. field magnitude F for the cases of waves present and waves absent. A total of 2633.7 hours of data without waves and 595.9 hours of data with waves was used. The distributions are quite similar with a slight enhancement in the distribution with waves at 8γ being the most obvious difference between the two. The distributions closely resemble interplanetary distributions of IMP I (Ness, 1969) and IMP II (Fairfield and Ness, 1967) with a slight shift towards higher values on Explorer 34 possibly due to the new sunspot cycle. The similarity of the distributions in Figure 10 with and without waves indicates that the distributions compiled from measurements on earlier spacecraft are representative of the undisturbed interplanetary medium in spite of the presence of .01-.05 Hz waves.

IV. THEORETICAL DISCUSSION

The solar wind flows past the earth and its standing bow shock with a velocity which is in the range 300-600 km/sec approximately 90% of the time. The waves discussed in this paper must have a velocity greater than the solar wind velocity in order to propagate into the upstream interplanetary region. Two alternate explanations for the presence of .01-.05 Hz waves in the interplanetary region are: (1) propagation of whistler waves into the upstream region; or (2) local generation of Alfvén waves through a resonant interaction with protons moving upstream from the bow shock.

Whistler Propagation

Tidman and Northrop (1968) have discussed the propagation of waves into the upstream region. They conclude that low frequency waves near the ion gyrofrequency, Ω_i , are unable to propagate upstream because they have Alfvén velocities which are usually less than 100 km/sec. Higher frequency whistler mode waves with $\omega \gg \Omega_i$ have velocities greater than the solar wind velocity and hence can be observed upstream. These whistler waves can be identified with 01-.05 Hz waves observed near and below Ω_i only if they can be doppler shifted to the necessary lower frequencies.

The well-known cold plasma dispersion relation for propagation parallel to B is

$$\frac{c^2 k^2}{\omega^2} = 1 - \frac{\omega_{pe}^2}{\omega(\omega \mp \Omega_e)} - \frac{\omega_{pi}^2}{\omega(\omega \pm \Omega_i)} \quad (1)$$

where the upper and lower signs are for right or left circularly polarized waves respectively and $\omega_{pe,i}^2 = \frac{4\pi n e^2}{m_{e,i}}$ and $\Omega_{e,i} = \frac{eB}{m_{e,i} c}$ for waves with $\omega \gg \Omega_i$

(1) simplifies to

$$\frac{c^2 k^2}{\omega^2} \approx \frac{-\omega_{pe}^2}{\omega \mp \Omega_e} \quad (2)$$

From (2) the wavelength λ can be written as

$$\lambda = \frac{2\pi}{k} \approx 2\pi c \left(\frac{|\Omega_e - \omega|}{\omega_e^2 \omega} \right)^{\frac{1}{2}} \quad (3)$$

An upper limit on λ can be obtained by evaluating (3) with $\omega_e = 10^5$ and $\omega = \frac{\Omega_e}{100} = 18\Omega_i$, which is a low value still satisfying $\omega \gg \Omega_i$. We then obtain $\lambda \approx 200\text{km}$.

If waves of this small wavelength are to be identified as very low frequency .01-.05 Hz waves, they must be propagating upstream in the earth's frame with nearly zero-phase velocity (i.e., they must be nearly standing waves). For the following reasons it seems unlikely that standing waves could be frequently present.

1) Varying solar wind conditions would make it unlikely that the wave velocities in the earth's frame would continually be just enough greater than the solar wind velocities to doppler shift the waves into the low frequency range where they are observed such a large percentage of the time.

2) Fields making various angles with the solar wind direction would result in different doppler shifts which would tend to move the frequency out of the range where it is observed. Propagation transverse to the solar wind would involve no doppler shift and the waves should be observed with $\omega \gg \Omega_1$. This is not the case since the waves are observed at lower frequencies even when the field is oriented transverse to the solar wind direction.

3) Such small wavelength waves would probably be appreciably damped far from the shock.

Local Generation

The fact that .01-.05 Hz waves are circularly polarized and have frequencies below Ω_1 suggests that they might be Alfvén waves. Although such waves cannot propagate upstream into the oncoming solar wind, they could be excited locally by particles moving upstream along field lines connecting to the shock through the mechanism of two-stream instability with the solar wind. The protons detected by Asbridge et al. (1968) and Frank (1968) could play this role.

Alfvén's waves have a group velocity $V_A = B / \sqrt{4\pi n m_i} \ll V_{sw}$ and thus could not propagate upstream against the solar wind. The frequency observed in the satellite frame for an Alfvén wave of wave number k will therefore be due primarily to convection of the wave past the observing spacecraft. The frequency observed by the spacecraft will then be

$$\omega_{SAT} = k V_{sw} \quad (4)$$

Energy is resonantly transferred to the wave by the energetic protons if the protons "see" the wave electric field, E_w , at their gyrofrequency; i. e., if

$$k(V_p + V_{sw}) = \Omega_i \quad (5)$$

or $V_p = V_{sw} \left(\frac{\Omega_i}{\omega_{SAT}} - 1 \right)$.

The quantity Ω_i / ω_{SAT} is observed to generally be of the order of 3 with ω_{SAT} increasing when Ω_i increases so that the ratio tends to be constant. This gives proton velocities on the order $V_p \approx 2 V_{sw}$ corresponding to 2 keV protons which is a frequently observed energy. Under the local acceleration hypothesis the $2.7 V_{sw}$ velocity derived in this paper is interpreted as a proton velocity. The value agrees well with the proton velocities that are observed and those that are needed to resonate with the waves.

The sense of rotation of E_w seen by the protons moving upstream must be the same as the rotation sense of a proton if resonant energy transfer is to occur. To an observer looking along a field line, protons gyrate counterclockwise which is in agreement with the predominant sense of rotation observed experimentally and illustrated in Figure 4.

V SUMMARY AND DISCUSSION

Magnetic field waves in the frequency range .01-.05 Hz have been found to be a common property of the interplanetary medium in the cislunar space surrounding the earth. It is concluded that the waves are associated with the presence of the earth's bow shock since they are seen only on field lines which intersect the shock. The waves are primarily transverse and amplitudes are typically 10-50% of the field magnitude. The amplitude decreases slowly with distance from the shock, probably by not more than a factor of 2 in a $15 R_E$ distance. Large amplitude waves often exhibit irregular waveforms and have broad spectral peaks, particularly in the frequency range .01- .05 Hz. Smaller amplitude waves are more likely to have coherent waveforms and sharper spectral peaks in this frequency range. The wave frequency depends on total field magnitude with higher frequencies corresponding to higher magnitudes. The spectral peaks in the spacecraft reference frame are always below the proton gyrofrequency.

The more coherent waves are usually circularly polarized. When one looks along the field which is oriented along the positive z axis of a right handed coordinate system, the disturbance vector rotates in the counterclockwise sense approximately 90% of the time. Occurrences of the opposite sense of rotation were infrequent and confined largely to one particular day.

Waves are seen more than 90% of the time when the magnetic field at the spacecraft intersects the shock at the proper orientation. This suggests that .01-.05 Hz transverse waves are a continually present feature of the solar wind-earth interaction with the waves constantly present on field lines intersecting the shock.

The absence of waves at particular field orientations where the field projection still intersects the shock is interpreted as due to there being insufficient time for propagation up a field line which is convecting toward the shock with the solar wind. From this observation the average wave velocity in the plasma frame is calculated as 2.7 ± 0.4 times the solar wind velocity.

Two alternate theoretical explanations are proposed to explain the presence of .01-.05 Hz waves: (1) propagation of whistler mode waves from the bow shock into the upstream medium; and (2) local generation of Alfvén waves through the mechanism of a two stream instability between the solar wind protons and protons moving back upstream from the earth's bow shock. If whistlers are to be identified as the .01-.05 Hz waves, they must be doppler shifted from $\omega \gg \Omega_i$ in the plasma frame to $\omega < \Omega_i$ in the spacecraft frame. The waves have relatively small ($\lambda \lesssim 200\text{km}$) wavelengths and it is suggested that this large doppler shift to the .01-.05 Hz frequency range is unlikely. Local generation of Alfvén waves appears to be a more attractive possibility.

The presence of large amplitude waves just outside the bow shock should also be considered in relation to bow shock studies. In spite of the fact that the waves do not obscure shock crossings by significantly increasing the field magnitude, they will tend to make some shock crossings less clear, particularly when the data sampling rate is low. This effect has undoubtedly contributed to occasional ambiguities in shock positions and to suggestions that there exist diffuse shock structures. The presence of waves at certain field orientations also emphasizes the possible importance of field orientation in the investigation of shock phenomena. It is now clear that studying sharply defined shock transitions associated with quiet interplanetary fields is equivalent to studying a class of shocks where the field tends to be transverse to the shock normal.

ACKNOWLEDGEMENTS

The author gratefully acknowledges the support and encouragement of Dr. Norman F. Ness who conceived and designed the Explorer 34 experiment and Mr. Joseph B. Seek who supervised the engineering aspects of the experiment. Appreciation is also expressed to Dr. D. A. Tidman for contributing many of the ideas expressed in the section of theoretical discussion. Helpful ideas and suggestions were also contributed by numerous other colleagues at Goddard Space Flight Center.

TABLE I

Orbit No.	ϕ_c	AB	AA'	$\frac{V_{w=AB}}{V_{swAA}}$
1-5	90°	8.0	4.0	2.0
6-10	65°	11.0	5.2	2.1
11-15	55°	11.0	4.3	2.6
16-20	45°	11.5	3.7	3.1
21-25	35°	11.0	3.5	3.1
26-30	30°	14.0	5.6	2.5
31-35	45°	12.0	4.0	3.0
36-40	55°	9.3	2.8	3.3
41-45	80°	7.7	2.7	2.9
45-50	95°	7.1	2.9	2.5
				<hr/> 2.7±.4

REFERENCES

- Anderson, K. A., Energetic Electrons of Terrestrial Origin
Upstream in the Solar Wind, J. Geophys. Res., 73, 2387-2397, 1968
- Asbridge, J. R., S. J. Bame, and I. B. Strong, Outward Flow of
Protons from the Earth's Bow Shock, J. Geophys. Res., 73,
5777, 1968
- Fairfield, D. H. and N. F. Ness, Magnetic Field Measurements with
IMP 2 Satellite, J. Geophys. Res., 72, 2379-2402, 1967
- Fan, C. Y., G. Gloeckler, and J. A. Simpson, Evidence for >30 keV
Electrons Accelerated in the Shock Transition Region Beyond
the Earth's Magnetospheric Boundary, Phys. Rev. Letters, 13,
149, 1964
- Fan, C. Y., G. Gloeckler, and J. A. Simpson, Acceleration of
Electrons near the Earth's Bow Shock and Beyond, J. Geophys.
Res., 71, 1837, 1966
- Frank, L. A. and W. L. Shope, A Cinematographic Display of
Observations of Low Energy Proton and Electron Spectra in the
Terrestrial Magnetosphere and Magnetosheath and in the
Interplanetary Medium, Abstract in Transaction of the America
Geophysical Union 49, 279, 1968
- Greenstadt, E. W., I. M. Green, G. T. Inouye, A. J. Hundhausen,
S. J. Bame, and I. B. Strong, Correlated Magnetic Field and
Plasma Observations of the Earth's Bow Shock. J. Geophys.
Res., 73, 51-60, 1968

- Heppner, J. P., M. Sugiura, T. L. Skillman, B. G. Ledley, and M. Campbell, OGO-A Magnetic Field Observations, J. Geophys. Res., 72, 5417-5471, 1967
- Jokipii, J. R., Correlation of ≥ 30 kev. Electron Pulses and Magnetic Fields in the Magnetosheath and Beyond, J. Geophys. Res., 73, 931-941, 1968
- Kawashima, Nobuki, Analysis of Fluxuation in the Magnetic Field Obtained by IMP II, GSFC Preprint X-616-68-271, July 1968
- Ness, N. F., C. S. Scarce, and J. B. Seek, Initial Results of the IMP I Magnetic Field Experiment, J. Geophys. Res., 69, 3531, 1964
- Ness, N. F., Direct Measurements of Interplanetary Magnetic Field and Plasma, To be published in Annals of the IQSY, 1969.
- Tidman, D. A., and T. G. Northrop, Emission of Plasma Waves by the Earth's Bow Shock, J. Geophys. Res., 73, 1543, 1968.
- Wolfe, J. H., R. W. Silva and M. A. Meyers, Observations of the Solar Wind During the Flight of IMP-I, J. Geophys. Res., 71, 1319, 1966.

FIGURE CAPTIONS

- Figure 1 Projection of Explorer 34 orbits in the solar ecliptic XY Plane (top) and YZ plane (bottom). The outer semi-circle in the top portion represents the $34 R_E$ apogee of Explorer 34 and the circled numbers designate the position of the apogee of the various orbits.
- Figure 2 Three components of the interplanetary magnetic field for a twenty minute interval when relatively coherent waves are present $14 R_E$ from the average shock position.
- Figure 3 Three components of the interplanetary magnetic field for a twenty minute interval when relatively incoherent waves are present near the bow shock.
- Figure 4 Polarization diagram for a 2 minute segment of the data shown in Figure 2. The average field is directed into the page and the sense of rotation is the usual one observed for fields of this orientation. Units are gammas.
- Figure 5 Typical interplanetary spectra for two intervals when bow-shock associated waves are present. The traces are offset by one decade in power so the increased spacing between the Y and Z traces is due to increased power in the transverse X and Y components. The enhanced power is centered in the typical .01-.05 Hz region below the proton gyrofrequency (vertical dashed line).

Figure 6 Percentage of the time that waves are observed as a function of latitude and longitude. The compilation of this figure involved the use of 392 hours of interplanetary data when the spacecraft was in the solar ecliptic longitude range 298° - 318° on orbits 36-40. The waves are seen to occur only when the field is oriented in the region surrounding the shock normal.

Figure 7 Relative occurrence of waves as a function of longitude for ten different satellite longitude regions corresponding to the orbits indicated on the figure. Horizontal bars represent the regions of angles of fields whose projection intersects the shock. Vertical dashed lines indicate the θ angle at which a field would be oriented perpendicular to the shock. Waves are always seen to occur on fields which intersect the shock as the longitude of the spacecraft moves from the dusk meridian (bottom) to the dawn meridian (top).

Figure 8 Diagram indicating the range of angles θ_w where waves are seen on orbits 36-40. θ_c represents a cutoff angle where the wave phenomena can just move along a field line from B to A while the field is convected to position B'A'.

Figure 9 Explorer 33 data taken $46 R_E$ from the average shock position. Data are shown to illustrate the great distances at which bow-shock associated waves can be found.

Figure 10 Interplanetary field magnitude distribution in half gamma intervals for two sets of data separated according to whether waves are present or absent.

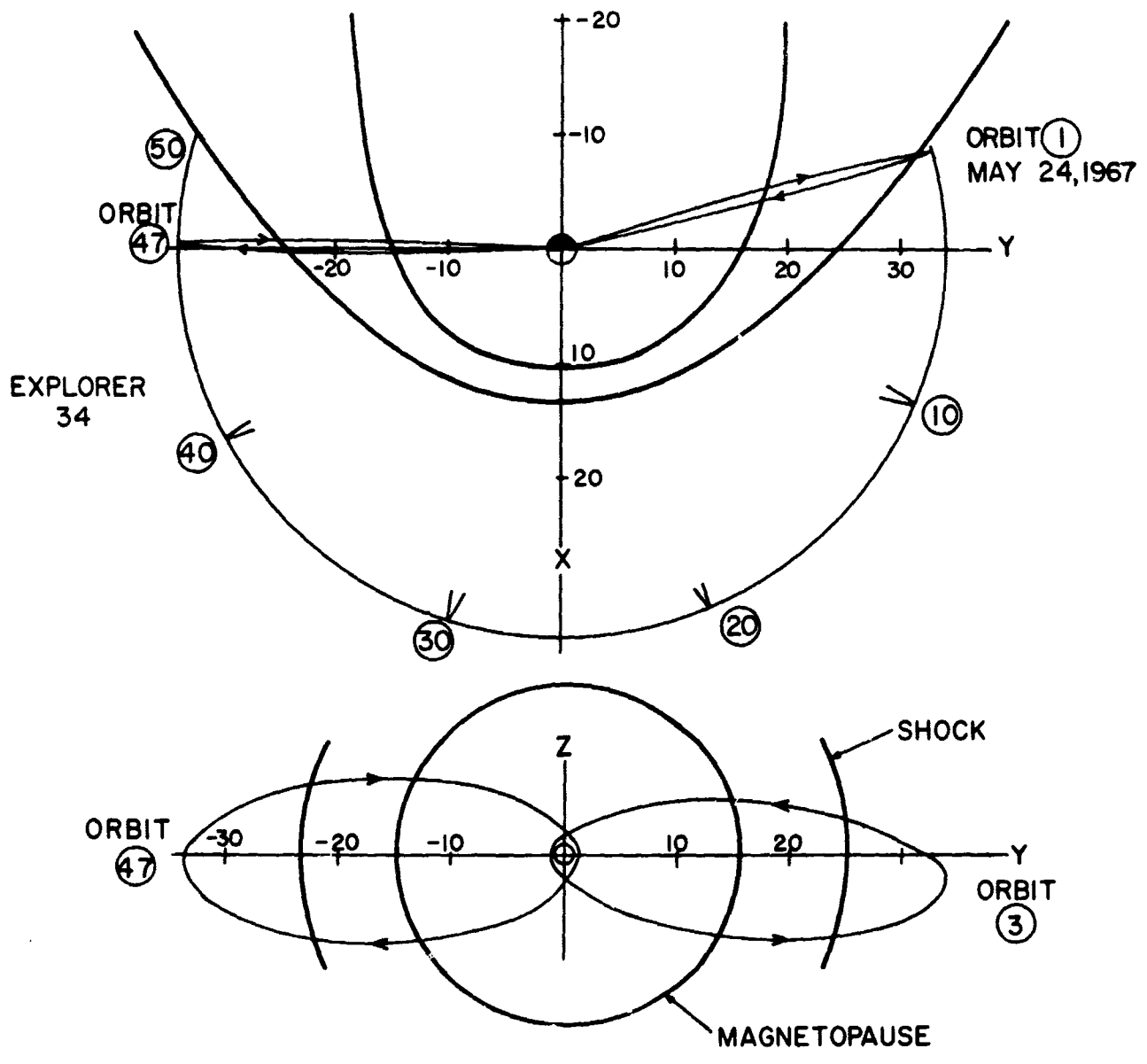
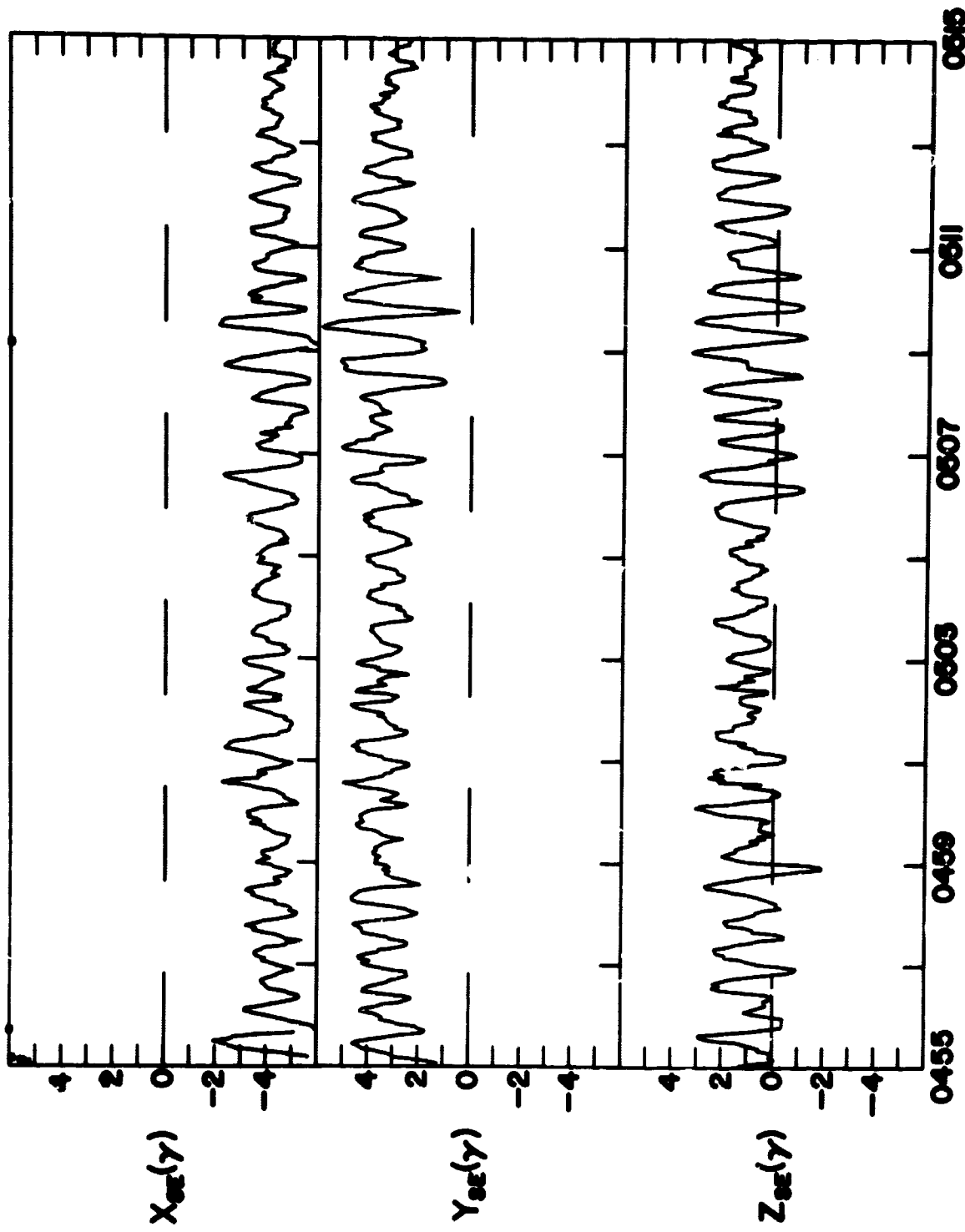
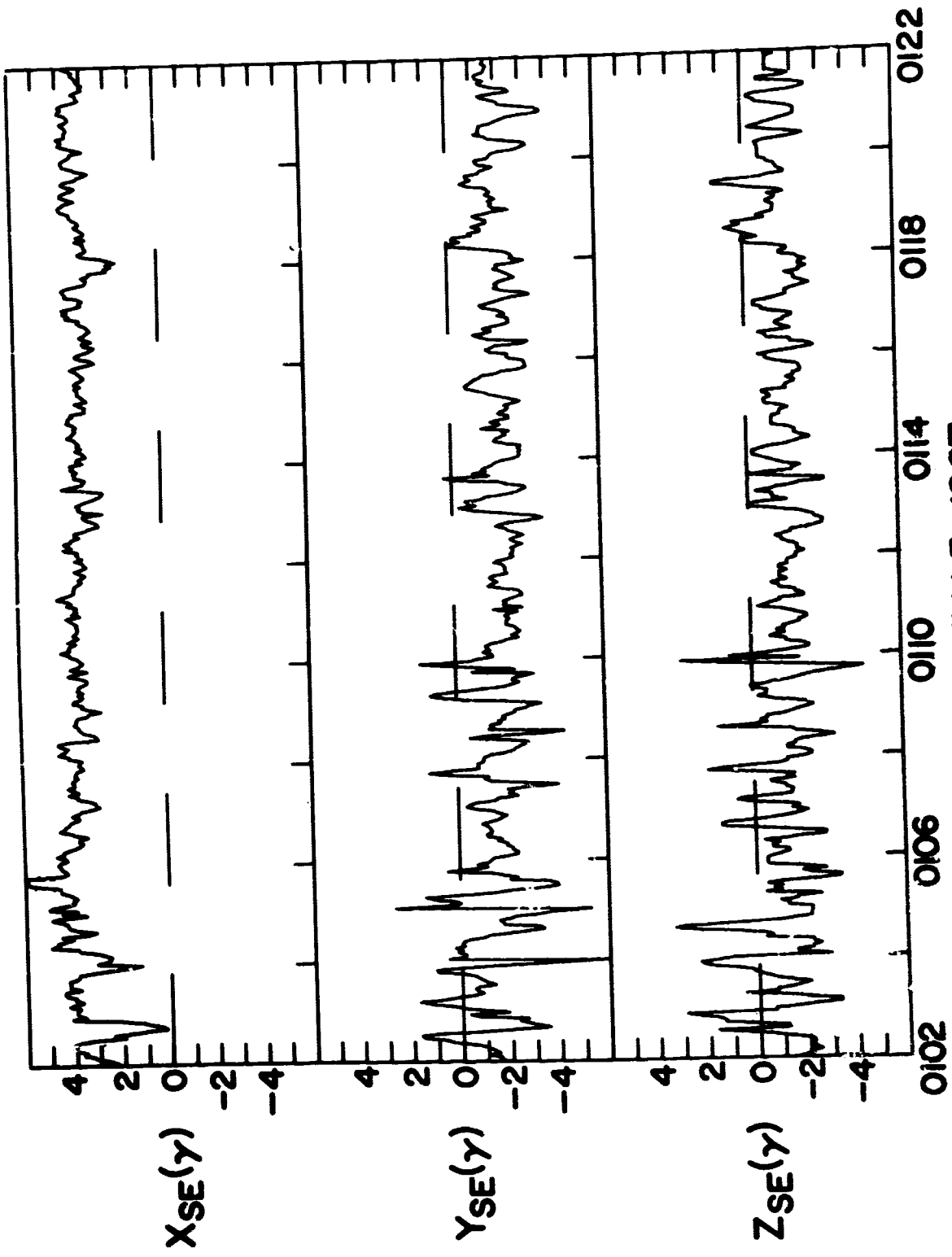


FIGURE 1



OCT. 26, 1967

FIGURE 2



JULY 3, 1967

FIGURE 3

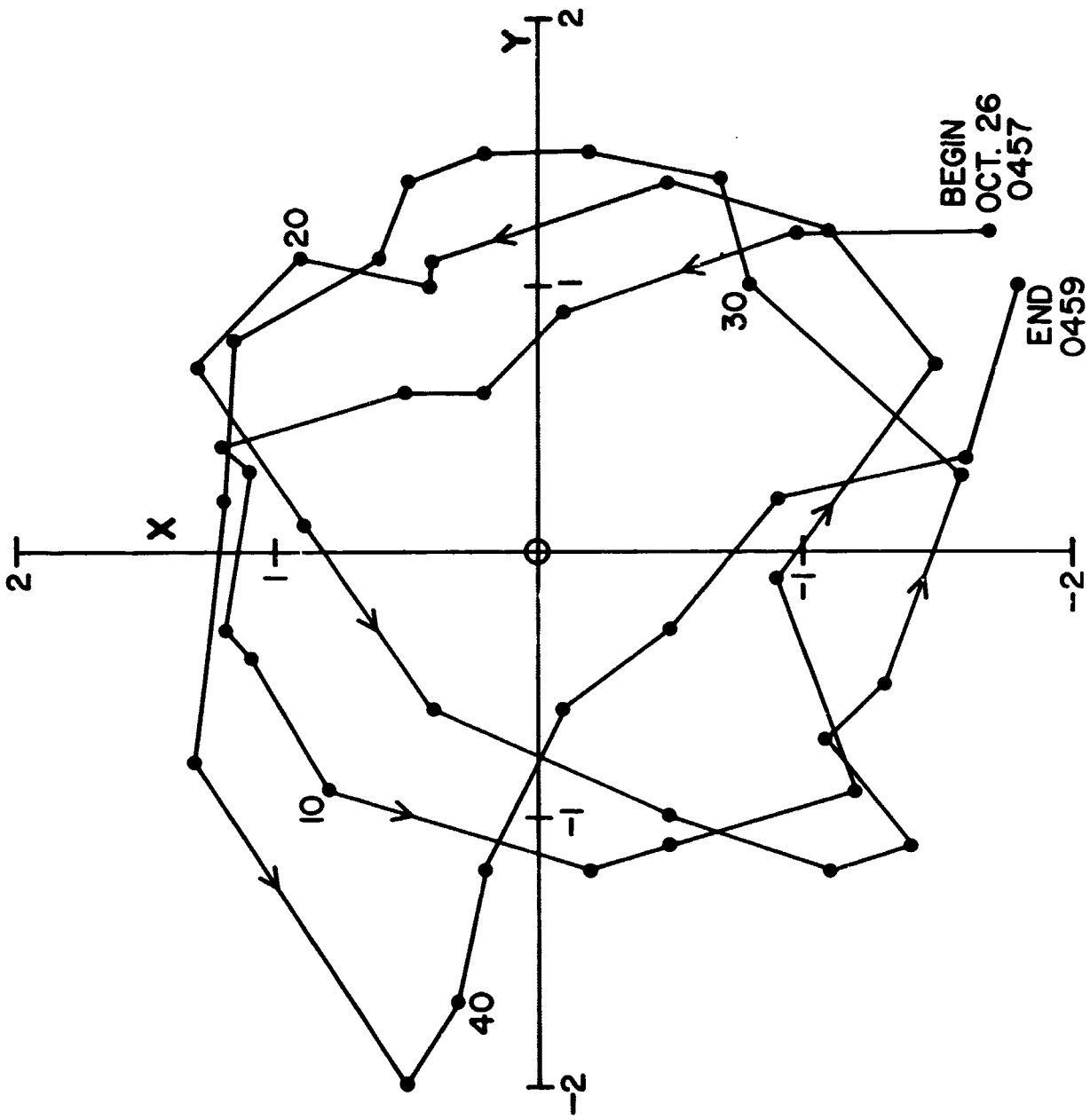


FIGURE 4

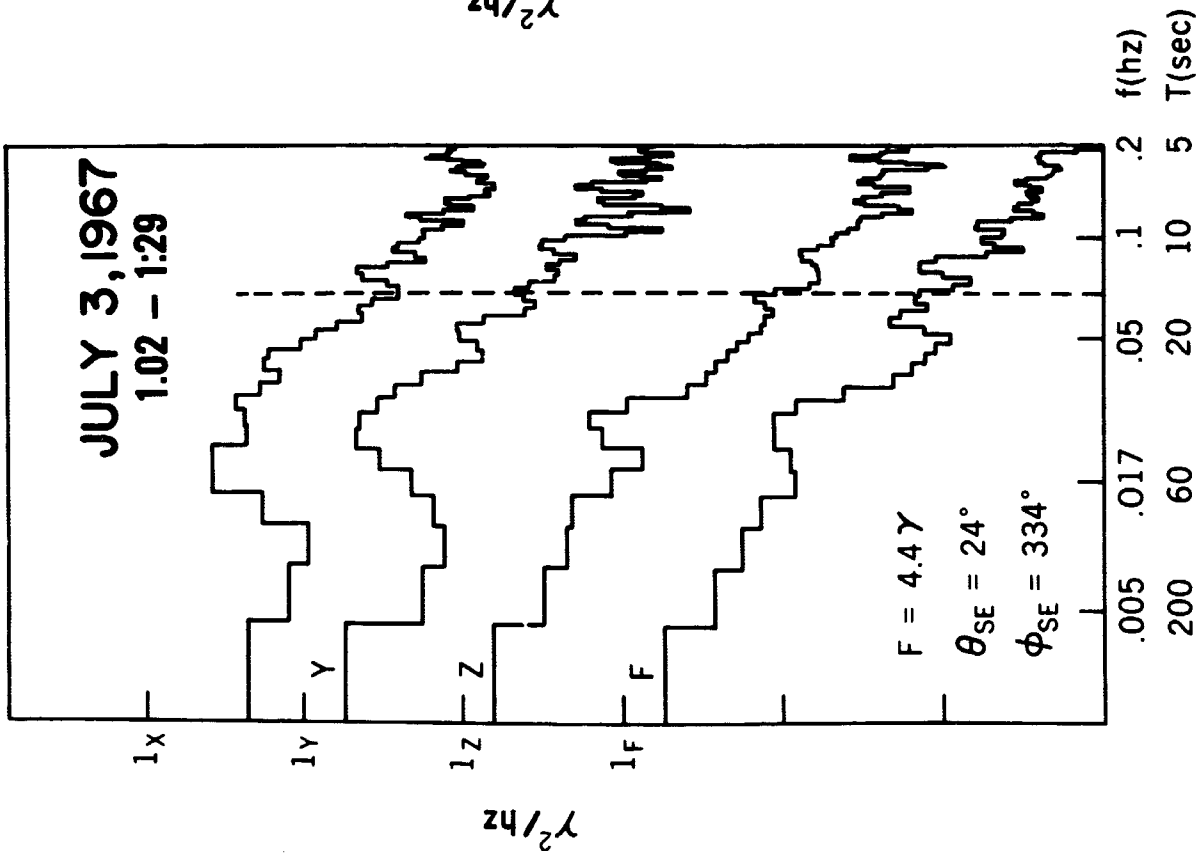
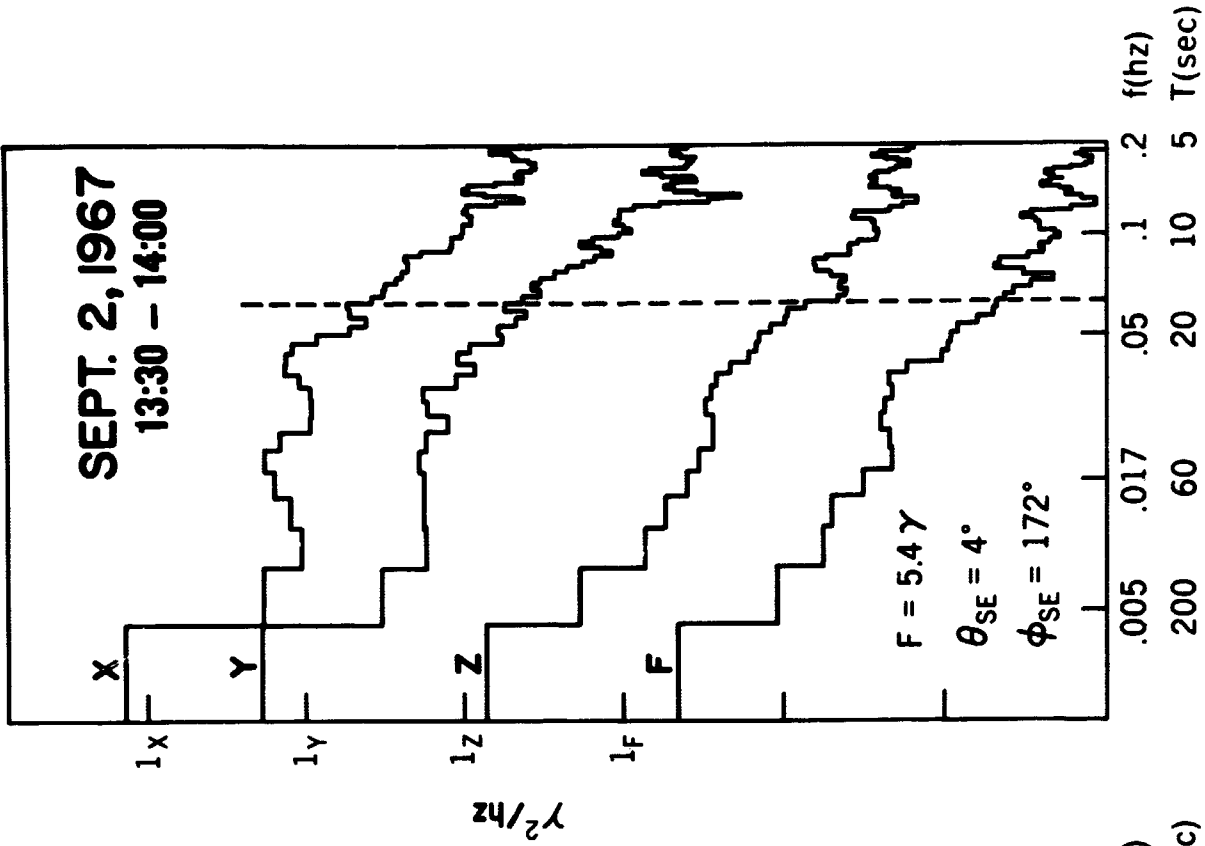
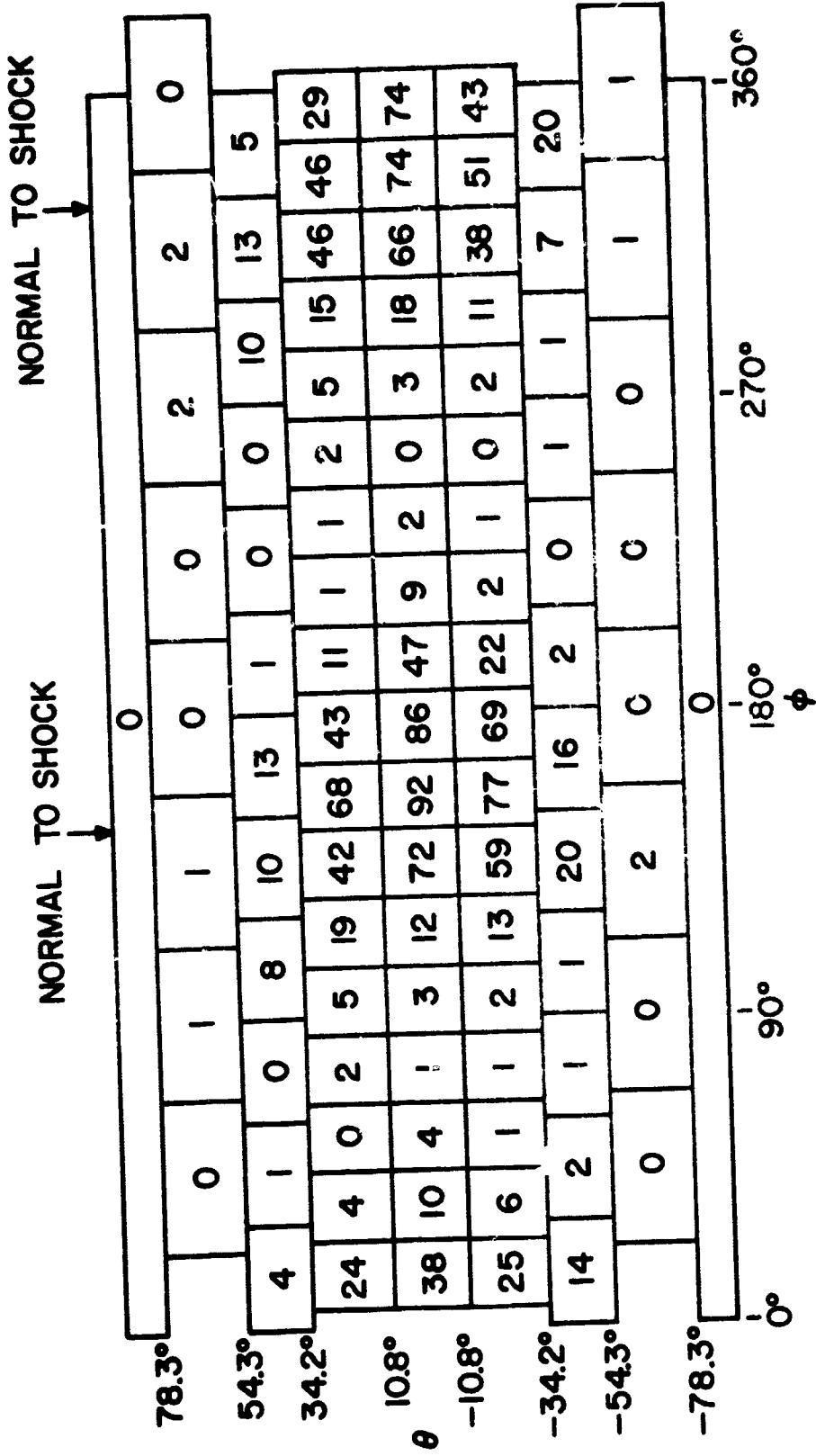


FIGURE 5



% WAVE OCCURRENCE - ORBITS 36 - 40

FIGURE 6

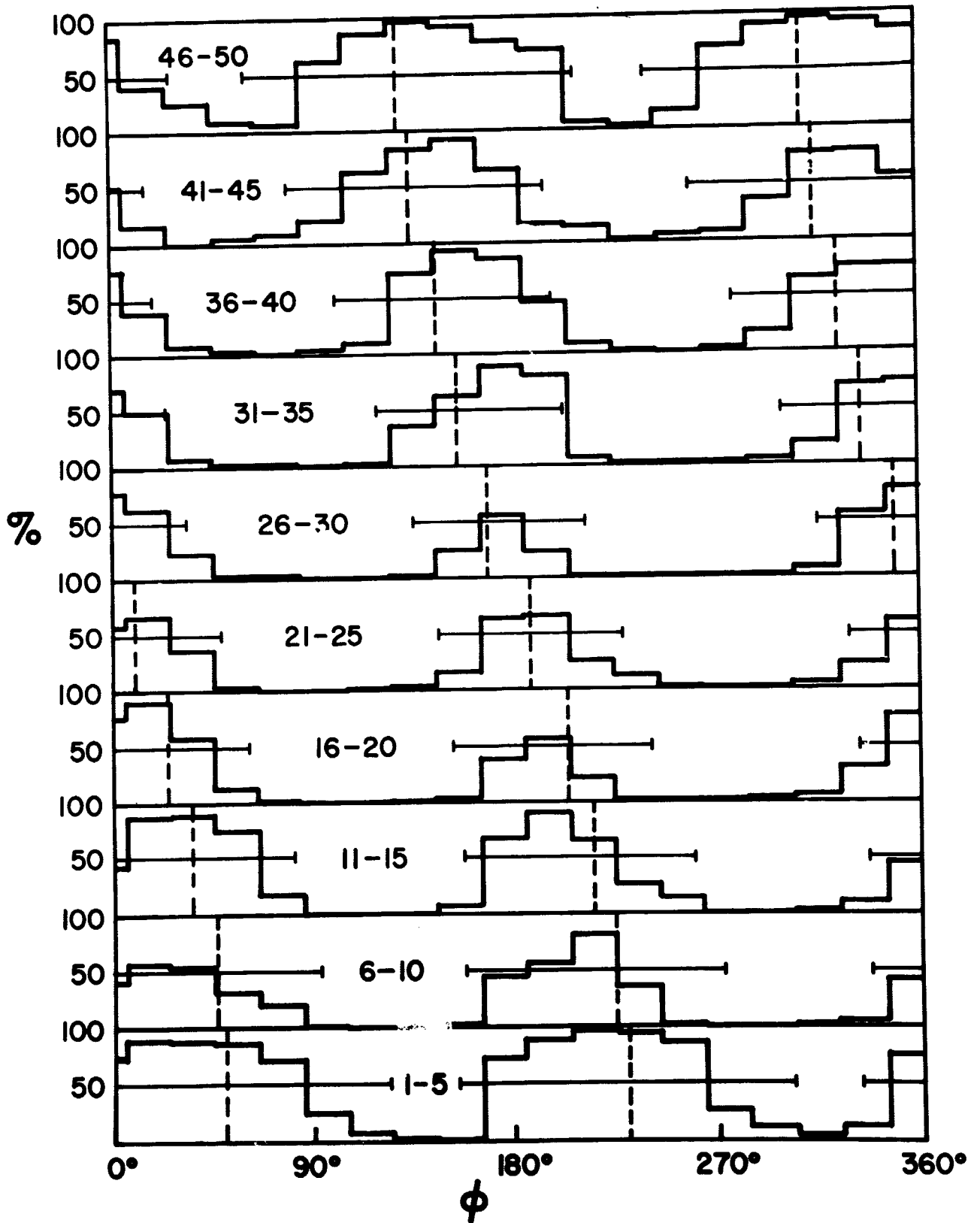


FIGURE 7

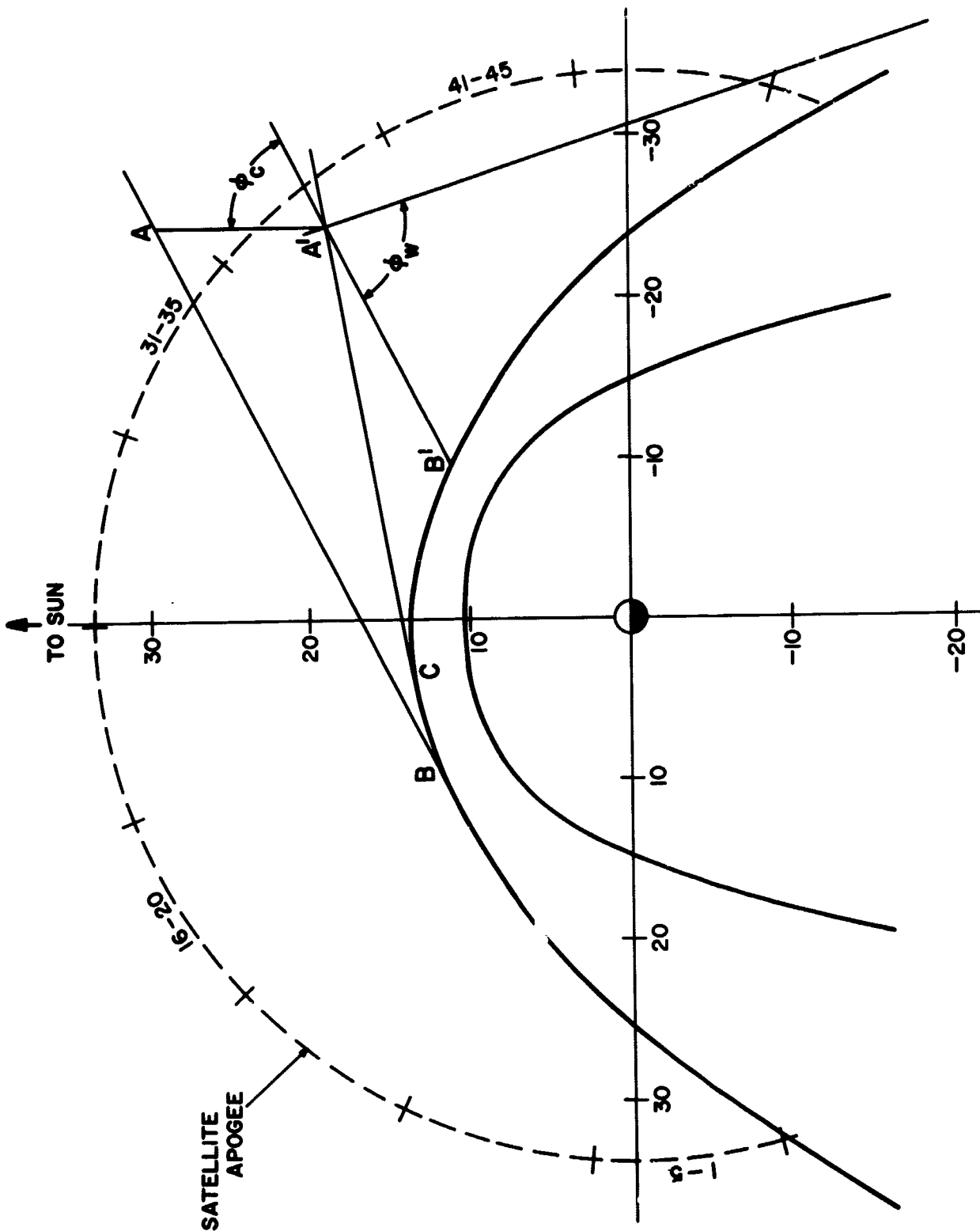
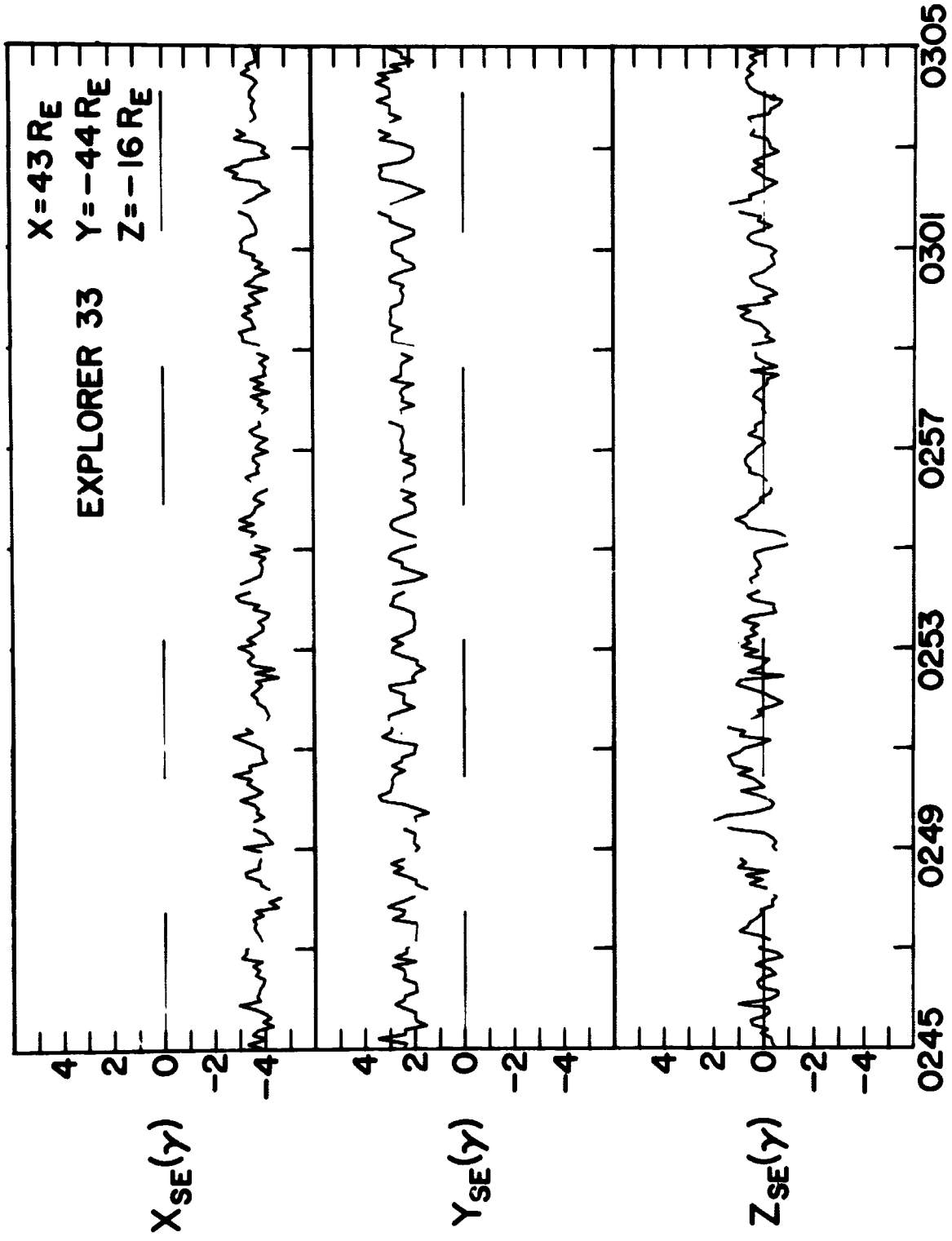


FIGURE 8



FEB 19, 1967

FIGURE 9

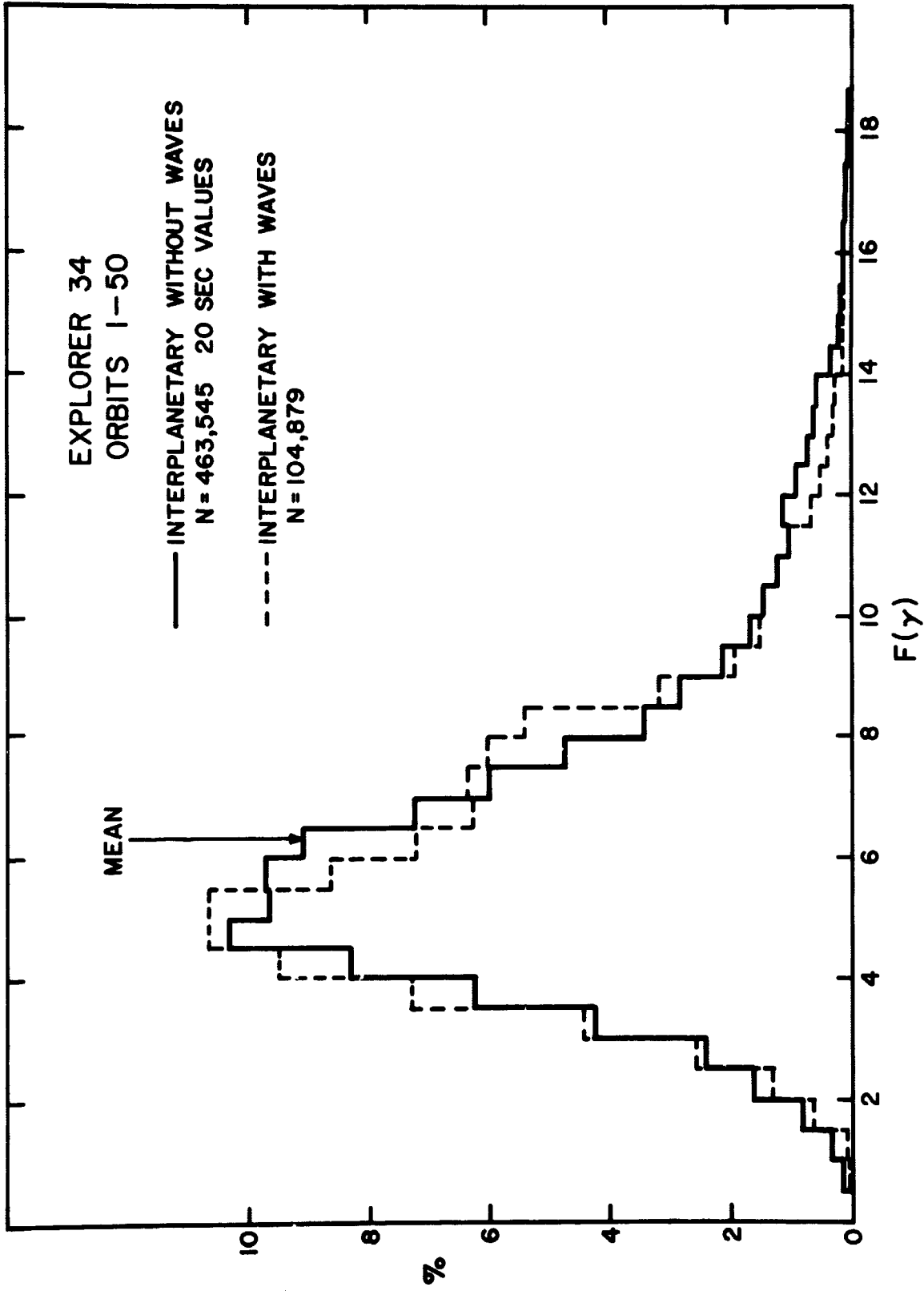


FIGURE 10